

# Atorvastatin overcomes gefitinib resistance in KRAS mutant human non-small cell lung carcinoma cells

J Chen<sup>1,9</sup>, H Bi<sup>2,3,9</sup>, J Hou<sup>2,4,9</sup>, X Zhang<sup>4</sup>, C Zhang<sup>4</sup>, L Yue<sup>4</sup>, X Wen<sup>4</sup>, D Liu<sup>4</sup>, H Shi<sup>2</sup>, J Yuan<sup>5</sup>, J Liu<sup>\*,6</sup> and B Liu<sup>\*,7,8</sup>

The exact influence of statins on gefitinib resistance in human non-small cell lung cancer (NSCLC) cells with KRAS mutation alone or KRAS/PIK3CA and KRAS/PTEN comutations remains unclear. This work found that transfection of mutant KRAS plasmids significantly suppressed the gefitinib cytotoxicity in Calu3 cells (wild-type KRAS). Gefitinib disrupted the Kras/PI3K and Kras/Raf complexes in Calu3 cells, whereas not in Calu3 KRAS mutant cells. These trends were corresponding to the expression of pAKT and pERK in gefitinib treatment. Atorvastatin (1  $\mu$ M) plus gefitinib treatment inhibited proliferation, promoted cell apoptosis, and reduced the AKT activity in KRAS mutant NSCLC cells compared with gefitinib alone. Atorvastatin (5  $\mu$ M) further enhanced the gefitinib cytotoxicity through concomitant inhibition of AKT and ERK activity. Atorvastatin could interrupt Kras/PI3K and Kras/Raf complexes, leading to suppression of AKT and ERK activity. Similar results were also obtained in comutant KRAS/PTEN or KRAS/PIK3CA NSCLC cells. Furthermore, mevalonate administration reversed the effects of atorvastatin on the Kras/Raf and Kras/PI3K complexes, as well as AKT and ERK activity in both A549 and Calu1 cells. The *in vivo* results were similar to those obtained *in vitro*. Therefore, mutant KRAS-mediated gefitinib insensitivity is mainly derived from failure to disrupt the Kras/Raf and Kras/PI3K complexes in KRAS mutant NSCLC cells. Atorvastatin overcomes gefitinib resistance in KRAS mutant NSCLC cells irrespective of PIK3CA and PTEN statuses through inhibition of HMG-CoA reductase-dependent disruption of the Kras/Raf and Kras/PI3K complexes.

*Cell Death and Disease* (2013) 4, e814; doi:10.1038/cddis.2013.312; published online 26 September 2013

**Subject Category:** Cancer

The epidermal growth factor receptor tyrosine kinase inhibitor (TKI), gefitinib (Iressa), benefits certain patients with non-small cell lung cancer (NSCLC). KRAS encodes a small GTP-binding protein involved in many cellular processes including proliferation, differentiation, and apoptosis.<sup>1</sup> Wild-type (WT) Kras protein has intrinsic GTPase activity that catalyzes the hydrolysis of bound GTP to GDP, thereby inactivating the growth-promoting signaling. KRAS mutations are detected in more than 25% of lung adenocarcinomas, 97% of which affect codon 12 or 13.<sup>2</sup> These mutations lead to locking of oncogenic Kras into the GTP-bound state, impairing GTPase activity and resultant constitutive activating RAS signaling. Mutational activation of KRAS is associated with primary resistance of gefitinib.<sup>2</sup> However, the exact mechanisms underlying mutant KRAS-mediated gefitinib resistance in NSCLC remain unclear. Besides, the development of clinically effective Kras-directed treatment in cancer therapies has been largely unsuccessful.<sup>3</sup>

Other somatic mutations also confer gefitinib resistance. Persistent activation of PI3K signaling by the PIK3CA oncogenic mutation is sufficient to abrogate gefitinib-induced apoptosis of NSCLC cells.<sup>4</sup> Activation of AKT signaling due to PTEN loss-of-function mutation also confers acquisition of resistance to gefitinib in NSCLC cells.<sup>5</sup> KRAS mutation has been found to frequently co-occur with PTEN loss-of-function mutation<sup>6</sup> or PIK3CA mutation<sup>7</sup> in lung cancer cells. However, whether KRAS/PTEN or KRAS/PIK3CA comutants influence gefitinib efficacy remains unknown.

Statins, HMG-CoA reductase inhibitors, reduce the synthesis of isoprenoids, geranylgeranyl-pyrophosphate, and their precursor mevalonate, which are essential substrates for posttranslational modifications of RAS.<sup>8</sup> The antitumor activity of statins has been suggested in various cancer cells including NSCLC cells.<sup>9</sup> Furthermore, previous studies show that statins enhance the tumor-inhibitory effect of many antitumor drugs, such as cetuximab in KRAS mutant human colorectal

<sup>1</sup>State Key Laboratory of Molecular Oncology, Cancer Institute and Hospital, Chinese Academy of Medical Sciences and Peking Union Medical College, Beijing 100191, China; <sup>2</sup>Lung Cancer Research Institute of Qiqihar Medical University, Heilongjiang 161009, China; <sup>3</sup>The Public and Health Institute of Wuhan University, Hubei 430072, China; <sup>4</sup>Cell and Molecular Biology Laboratory of Qiqihar Medical University, Heilongjiang 161009, China; <sup>5</sup>Department of Biochemistry and Molecular Biology, Peking University Health Science Center, Beijing 100191, China; <sup>6</sup>Medicine and Drug Research Institute of Qiqihar Medical University, Heilongjiang 161009, China; <sup>7</sup>Department of Pharmacology, School of Pharmacy, Guangdong Pharmaceutical University, Guangzhou 510006, China and <sup>8</sup>Guangdong Key Laboratory of Pharmaceutical Bioactive Substances, Guangdong Pharmaceutical University, Guangzhou, Guangdong 510006, China

\*Corresponding author: J Liu, Medicine and Drug Research Institute of Qiqihar Medical University, Heilongjiang 161009, China. Tel: +86-452-2663103; Fax: +86-452-2663701; E-mail: liujicheng@qmu.edu.cn

or B Liu, Department of Pharmacology, School of Pharmacy, Guangdong Pharmaceutical University, Guangzhou 510006, China. Tel: +86 20 36352128; Fax: +86 20 36352128; E-mail: liubing52000@163.com

<sup>9</sup>These authors contributed equally to this work.

**Keywords:** gefitinib; atorvastatin; mutant KRAS; NSCLC

**Abbreviations:** NSCLC, non-small cell lung cancer; TKI, tyrosine kinase inhibitor; DAB, diamino benzidine

Received 21.5.13; revised 17.7.13; accepted 29.7.13; Edited by M Agostini

cancer<sup>10</sup> and celecoxib in prostate cancers.<sup>11</sup> Our previous study also indicates that atorvastatin sensitizes NSCLC cells to carboplatin through inhibition of AKT activation.<sup>12</sup> However, the exact influence of statins on gefitinib resistance in KRAS mutant NSCLC cells remains unclear.

This study was designed to explore the mechanism underlying gefitinib resistance and the effect of atorvastatin on gefitinib sensitivity in KRAS mutant NSCLC cells. The results indicate that gefitinib fails to disrupt the direct interaction of Kras with PI3K and Raf, contributing to its resistance in KRAS mutant NSCLC cells. Our data also

suggest that atorvastatin can overcome gefitinib resistance in NSCLC cells harboring KRAS mutation irrespective of PIK3CA or PTEN status.

## Results

**Mutant KRAS-mediated PI3K and Raf pathway is critical for gefitinib resistance.** To confirm whether mutant KRAS is critically involved in gefitinib resistance in NSCLC, we treated Calu3 parental cells and its KRAS mutant counterpart with gefitinib for 3 days. Figure 1a showed that gefitinib

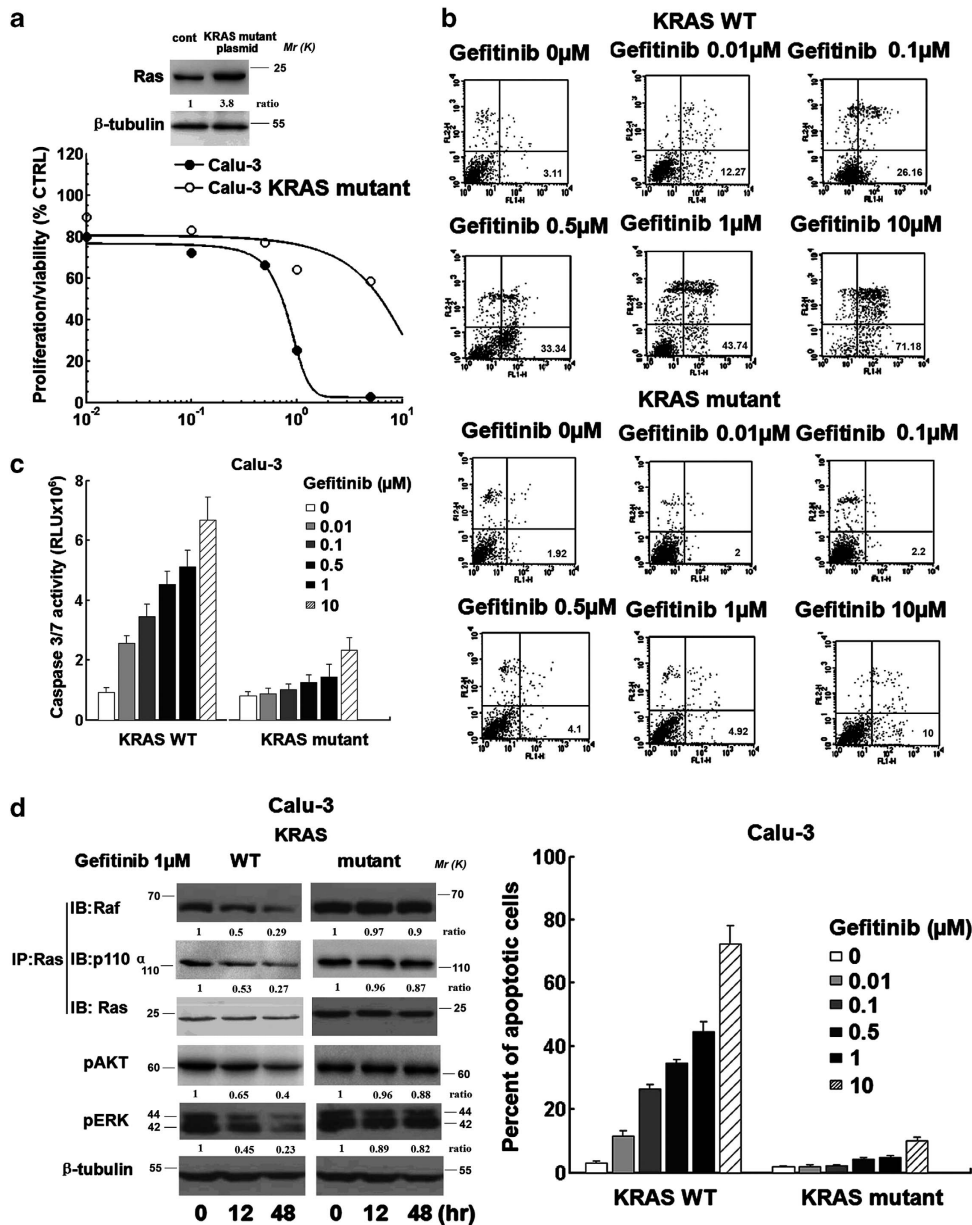


**Figure 1** Effect of gefitinib on the tumor growth of Calu3 cell and its KRAS mutant counterpart. (a–c) Gefitinib dose response. NSCLC cells were grouped to Calu3 and Calu3<sup>KRAS G12V</sup>. Proliferation/viability was analyzed after 3 days of treatment by MTT assay (a). Cell apoptosis was evaluated by flow cytometry assay (b) and caspase 3/7 activity assay (c). (d) Calu3 and Calu3<sup>KRAS G12V</sup> cells were treated with 1  $\mu$ M gefitinib for 0–48 h, then lysates were immunoprecipitated by using anti-Kras antibody and analyzed for coimmunoprecipitating p110 $\alpha$  and Raf by means of western blotting, and then pAKT and pERK levels were analyzed using western blotting,  $\beta$ -tubulin was used as the protein loading control. Bars are mean  $\pm$  S.D. from three independent experiments

treatment effectively inhibited Calu3 cell growth with the  $IC_{50}$  value of  $0.43 \mu\text{M}$ . Transfection of mutant KRAS plasmids could significantly suppress the gefitinib cytotoxicity with the  $IC_{50}$  value of gefitinib increased to  $4.2 \mu\text{M}$ . The transfection efficacy of pBABE-puro plasmid (control plasmid) or pBabe puro-KRAS G12V plasmid (KRAS mutant plasmid) was determined by means of western blotting (Figure 1a). As shown in Figures 1b and c, gefitinib dose dependently increased the apoptotic rate and caspase 3/7 activity in Calu3 parental cells, whereas exerted minimal or low effects in KRAS mutant Calu3 cells.

Next, we sought to explore the mechanism underlying mutant KRAS-mediated gefitinib resistance in NSCLC cells. As shown in Figure 1d,  $1 \mu\text{M}$  gefitinib time dependently inhibited the expression of pAKT and pERK in Calu3 cells. However, such inhibitory effect was absent in the presence of mutant KRAS plasmids (the right panel of Figure 1d). The results also showed that  $1 \mu\text{M}$  gefitinib time dependently disrupted the Kras/PI3K subunit p110 $\alpha$  and Kras/Raf complexes in Calu3 cells, whereas not in Calu3 KRAS mutant cells. These trends were corresponding to the expression of pAKT and pERK in gefitinib treatment. Mutant Kras directly binds to Raf proteins and the PI3K subunit p110 $\alpha$ , leading to constitutive activation of both the MEK/ERK and PI3K/AKT pathways. Furthermore, as gefitinib exerts antitumor activity mainly via blockage of the MEK/ERK and PI3K/AKT signaling pathways,<sup>13</sup> the above results suggest that mutant KRAS-mediated gefitinib insensitivity was mainly derived from failure to disrupt the Kras/Raf and Kras/PI3K complexes in KRAS mutant NSCLC cells.

**Antitumor effect of atorvastatin and gefitinib on KRAS mutant NSCLC cells *in vitro*.** As shown in Figure 2a, clinical dose of atorvastatin ( $1 \mu\text{M}$ ) could effectively decrease the  $IC_{50}$  value of gefitinib from  $8.8$  to  $1.5 \mu\text{M}$  in A549 cells. Combination of  $5 \mu\text{M}$  atorvastatin and gefitinib worked synergistically and more effectively than gefitinib in the presence of  $1 \mu\text{M}$  atorvastatin. Similar results were also obtained in Calu1 cells.

Activating PIK3CA mutation also confers RTK inhibitor resistance. To demonstrate whether comutant KRAS/PIK3CA mediates gefitinib resistance in NSCLC treatment, the H460 NSCLC cell line harboring comutant KRAS/PIK3CA was chosen. As shown in Figure 2a, the  $IC_{50}$  value of gefitinib in H460 treatment was  $16.4 \mu\text{M}$ , which was higher than that in A549 or Calu1 treatment, suggesting that comutant KRAS/PIK3CA might further decrease the chemosensitivity of gefitinib. Atorvastatin could still enhance gefitinib efficacy in H460 cells (gefitinib treatment *versus*  $1$  or  $5 \mu\text{M}$  atorvastatin + gefitinib treatment,  $IC_{50} = 16.4$  *versus*  $4.06$  or  $1 \mu\text{M}$ ). Besides, we transfected PI3K mutation plasmid-PIK3CA (E545K) into A549 and Calu1 cells. As shown in Figures 2b and d, atorvastatin could also enhance the gefitinib efficacy in these transfected cells, confirming that atorvastatin can sensitize NSCLC cells to gefitinib in the presence of comutant KRAS/PIK3CA.

PTEN loss-of-function mutation is another critical factor causing RTK inhibitor resistance. The H157 NSCLC cell line harboring comutant KRAS/PTEN was chosen to observe the gefitinib resistance. As shown in Figure 2a (curve lines), atorvastatin dose dependently enhanced gefitinib efficacy in

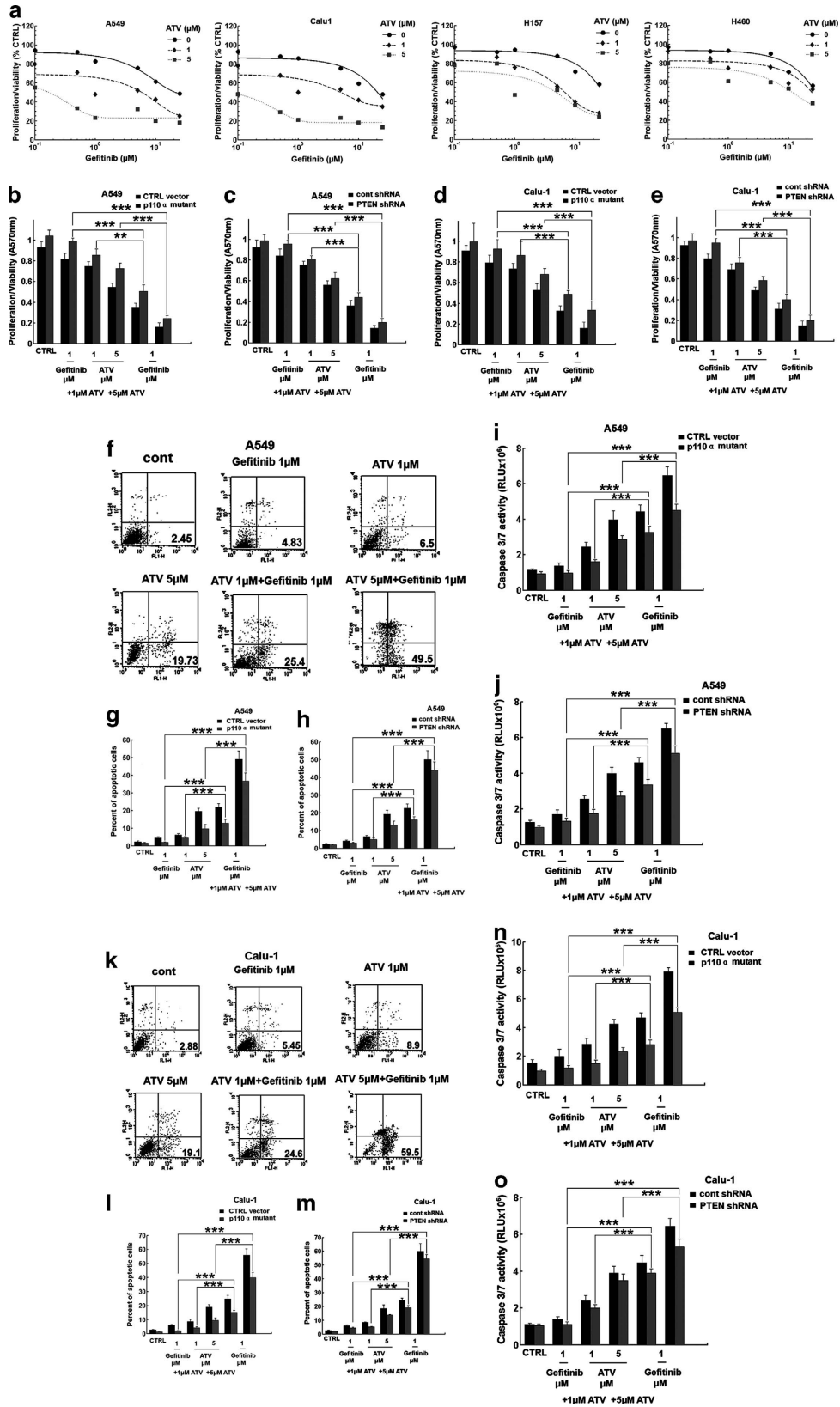
comutant KRAS/PTEN H157 cells (gefitinib treatment *versus*  $1$  or  $5 \mu\text{M}$  atorvastatin + gefitinib treatment,  $IC_{50} = 18$  *versus*  $2.08$  or  $0.71 \mu\text{M}$ ). As shown in Figures 2c and e, although mutant PTEN increased the gefitinib concentration required for inhibition of proliferation of KRAS mutant NSCLC cells (A549 and Calu1 cells), addition of  $1$  or  $5 \mu\text{M}$  atorvastatin could sensitize comutant KRAS/PTEN NSCLC cells to gefitinib compared with each agent alone.

To investigate the effect of the atorvastatin–gefitinib combination on apoptosis of NSCLC cells, A549 cells were treated for 48 h with atorvastatin and gefitinib alone or their combination. As shown in Figure 2f, atorvastatin alone dose dependently increased the apoptotic rate in A549 treatment assayed by flow cytometry analysis. However,  $1 \mu\text{M}$  gefitinib alone could partially induce apoptosis of A549 cells. Combining atorvastatin and gefitinib could produce more apoptotic rate than each agent alone, and  $5 \mu\text{M}$  atorvastatin–gefitinib combination worked more effectively than gefitinib in the presence of  $1 \mu\text{M}$  atorvastatin.

We then observed whether atorvastatin enhanced the proapoptotic effect of gefitinib in A549 cells with the comutant KRAS/PIK3CA or KRAS/PTEN by flow cytometry assay. As shown in Figures 2g and h, atorvastatin could still dose dependently increase the apoptotic rate of these two A549 cells (comutant KRAS/PIK3CA or KRAS/PTEN) and sensitize these cells to gefitinib treatment. A similar increase in caspase 3/7 activity was reflected in the apoptotic index of A549 parental cell, or its other two mutant status, suggesting that the addition of atorvastatin significantly enhances the same concentration of gefitinib for reaching the threshold of caspase activation and apoptosis in KRAS mutant alone, or in the comutant KRAS/PIK3CA or KRAS/PTEN status of A549 cells (Figures 2i and j). Similar results were also obtained in another NSCLC cell line Calu1 and its KRAS/PIK3CA or KRAS/PTEN comutants (Figures 2k, l, m, n and o).

**Atorvastatin and gefitinib synergistically inhibit the PI3K/AKT and MEK/ERK pathways.** Next we explored the mechanisms underlying atorvastatin-mediated increase in gefitinib sensitivity in KRAS mutant NSCLC cells. The PI3K inhibitor-LY294002 and MEK inhibitor-PD98509 were chosen, and whether they could enhance the tumor-inhibitory effect of gefitinib in A549 and Calu1 parental cells and their KRAS/PIK3CA or KRAS/PTEN comutants was subsequently observed.

As shown in Figure 3a, LY294002 ( $30 \mu\text{M}$ ) or PD98509 ( $30 \mu\text{M}$ ) alone inhibited A549 cell proliferation by  $44.66$  or  $33.07\%$ , respectively. Additional administration of LY294002 ( $30 \mu\text{M}$ ) or PD98509 ( $30 \mu\text{M}$ ) enhanced the tumor-inhibitory effect of gefitinib ( $1 \mu\text{M}$ ) from  $11.76$  to  $64.83$  or  $57.78\%$ , respectively. In comutant KRAS/PIK3CA and KRAS/PTEN statuses, LY294002 ( $30 \mu\text{M}$ ) or PD98509 ( $30 \mu\text{M}$ ) alone could still obtain  $38.83$  or  $31.76\%$  and  $36.18$  or  $38.48\%$  inhibitory rates. Additional administration of LY294002 ( $30 \mu\text{M}$ ) or PD98509 ( $30 \mu\text{M}$ ) could still enhance the tumor-inhibitory effect of gefitinib ( $1 \mu\text{M}$ ) from  $5.01$  to  $60.49\%$  or  $55.81$  and  $2.27$  to  $55.78$  or  $54.99\%$  in KRAS/PIK3CA or KRAS/PTEN comutants, respectively (Figures 3b and c). The similar results were also obtained in Calu1 cells and their KRAS/PIK3CA or KRAS/PTEN comutant (Figures 3a, b and c).



We further observed whether atorvastatin alone or combined with gefitinib inhibited the activation of AKT and ERK. As shown in Figures 3d, e and f, 1 or 5  $\mu$ M atorvastatin alone dose dependently inhibited the activation of AKT by 52.47 or 66.1% in A549 parental cells, by 46.5 or 61.33% in cells with comutant KRAS/PIK3CA, and by 50.5 or 63.9% in cells with comutant KRAS/PTEN. Additional administration of 1 or 5  $\mu$ M atorvastatin enhanced the inhibitory effect of gefitinib (1  $\mu$ M) on AKT activation in A549 parental cell and its KRAS/PIK3CA or KRAS/PTEN comutants (Figures 3d, e and f).

However, 1  $\mu$ M atorvastatin alone or combined with 1  $\mu$ M gefitinib could not induce the ERK inhibition of A549 cell and

its KRAS/PIK3CA or KRAS/PTEN comutant until the dose of atorvastatin was elevated to 5  $\mu$ M (Figures 3g, h and i). The similar AKT or ERK inhibitory effect mediated by atorvastatin alone or in the presence of 1  $\mu$ M gefitinib was also obtained in Calu1 cells and their KRAS/PIK3CA or KRAS/PTEN comutants (Figures 3g, h and i).

**Atorvastatin-induced inhibition of the PI3K/AKT and MEK/ERK pathways correlates with disruption of the Kras/Raf and Kras/PI3K complexes.** As shown in Figure 4a, immunostaining of A549 cells and Calu1 cells with Kras and PI3K p110 $\alpha$  antibodies revealed that Kras and

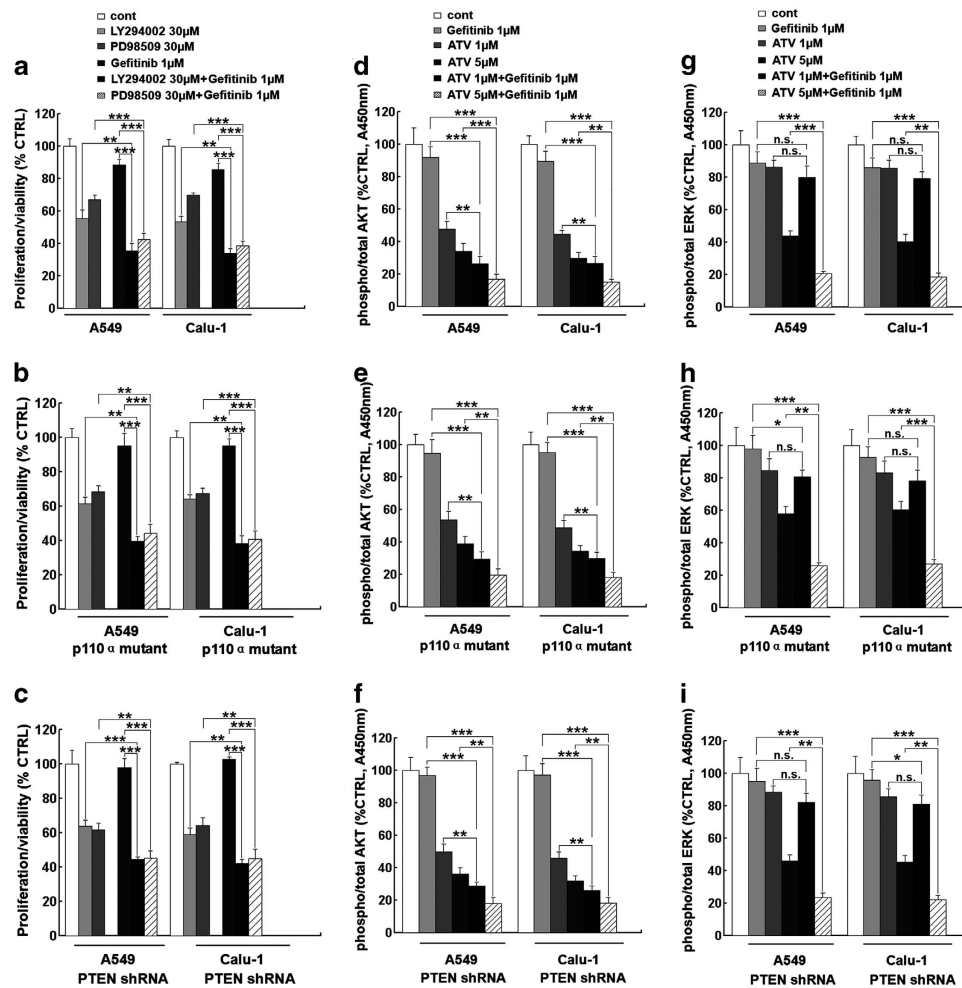


**Figure 3** Atorvastatin enhances the tumor-inhibitory effect of gefitinib in NSCLC cells through inhibiting AKT and ERK activation. (a–c) A549 and Calu1 parental cells (a) or their PIK3CA (b), and PTEN (c) mutants were treated with control solvent, 30  $\mu$ M LY294002, 30  $\mu$ M PD98509, 1  $\mu$ M gefitinib, or their combination, respectively. Cell proliferation/viability was determined by MTT assay after a 3-day incubation. (d–i) A549 and Calu1 cells (d and g) or their PIK3CA (e and h) and PTEN (f and i) mutants were treated with control solvent, 1  $\mu$ M gefitinib, or 1 or 5  $\mu$ M atorvastatin, and their combinations. The activations of AKT and ERK were evaluated by the ratio of pAKT to total AKT (d–f) and pERK to total ERK (g–i), and analyzed by ELISA after 48-hr treatment. Bars are mean  $\pm$  S.D. from three independent experiments. n.s., no significant difference. \* $P$  < 0.05; \*\* $P$  < 0.01; \*\*\* $P$  < 0.001

**Figure 2** Effects of atorvastatin and gefitinib alone or in combination on the growth and apoptosis of KRAS mutant NSCLC cells. (a) A549, Calu1, H157, and H460 cells were treated with the indicated concentrations of gefitinib or in the presence of 1 or 5  $\mu$ M atorvastatin. (b–e) A549 (b and c) and Calu1 (d and e) cells were transfected with p110 $\alpha$  E545K or control vector (b and d), or PTEN or control shRNA (c and e). After 24 h, cells were treated with indicated doses of atorvastatin or gefitinib, and their combinations for 3 days, then proliferation was measured by MTT assay. (f and k) A549 (f) and Calu1 (k) cells were treated with indicated doses of atorvastatin or gefitinib, and their combinations for 48 h, cell apoptosis was evaluated by FCM assay. (g–o) The apoptosis of A549 (g–j) and Calu1 (l–o) PIK3CA mutant (g, i, l, n) or PTEN (h, j, m, o) mutant cells were also evaluated by FCM assay (g, h, i, m) and caspase 3/7 activity assay (i, j, n, o), respectively. Bars are mean  $\pm$  S.D. from three independent experiments. \*\* $P$  < 0.01; \*\*\* $P$  < 0.001

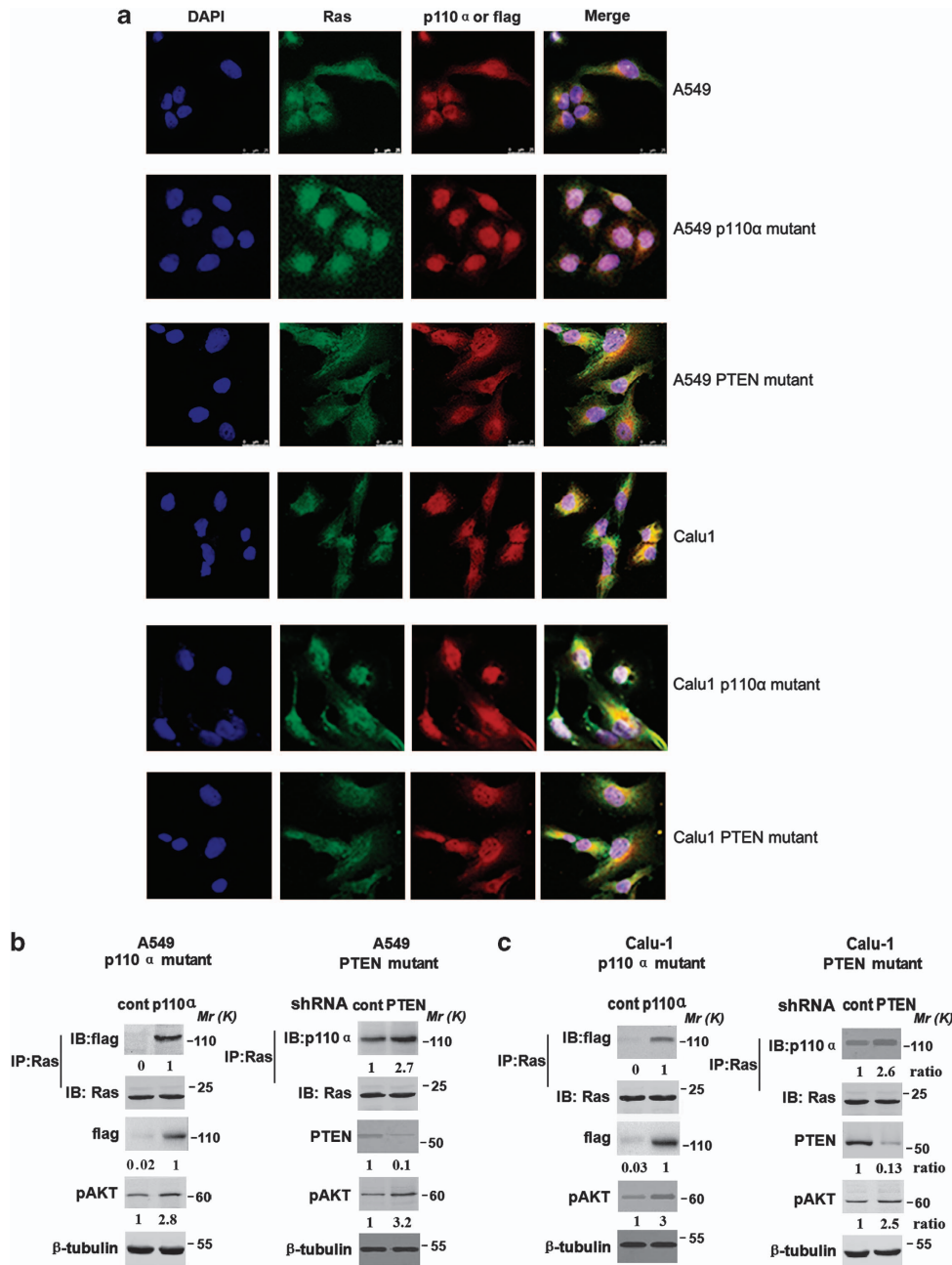


**Figure 4** Kras interacts with p110 $\alpha$  or its mutant status in NSCLC cells. (a) The interaction between Kras and p110 $\alpha$  was evaluated by confocal microscopy using anti-Kras, anti-p110 $\alpha$ , and anti-flag (evaluating Kras/ p110 $\alpha$  complex in A549 and Calu1 cells transfected with p110 $\alpha$  E545K plasmid) antibodies. Cells were also stained with DAPI to visualize the nucleus. One of the three to five similar experiments is shown. (b and c) The transfection efficacy of p110 $\alpha$  E545K or its control vector and PTEN or control shRNA and pAKT in A549 (b) and Calu1 (c) was evaluated using western blotting,  $\beta$ -tubulin was used as the protein loading control. Lysates were also immunoprecipitated by using anti-Kras antibody and analyzed for coimmunoprecipitating p110 $\alpha$  or flag antibody using western blotting

the PI3K p110 $\alpha$  subunit were well overlapped in these cells. Interestingly, when PIK3CA E545K plasmid or PTEN shRNA was transfected into these cells, Kras and p110 $\alpha$  were also well overlapped. To confirm that Kras directly interacts with the PI3K p110 $\alpha$  subunit in KRAS mutant cells irrespective of PIK3CA and PTEN statuses, we performed immunoprecipitation assay. As shown in Figure 4b, Kras directly bound with the PI3K p110 $\alpha$  subunit in A549 cells, and transfection with PIK3CA E545K plasmid or PTEN shRNA enhanced such

interaction corresponded with increased kinetics of the PI3K/AKT pathway. Consistent results were also obtained in another KRAS mutant cell line Calu1 (Figure 4c).

Next we sought to determine the mechanism underlying atorvastatin-induced inhibition of the PI3K/AKT pathway. As shown in Figure 5a, atorvastatin treatment led to a time-dependent dissociation of the PI3K p110 $\alpha$  subunit from Kras corresponded with inhibition of the PI3K/AKT pathway in A549 cells, as well as comutant KRAS/PIK3CA or KRAS/PTEN

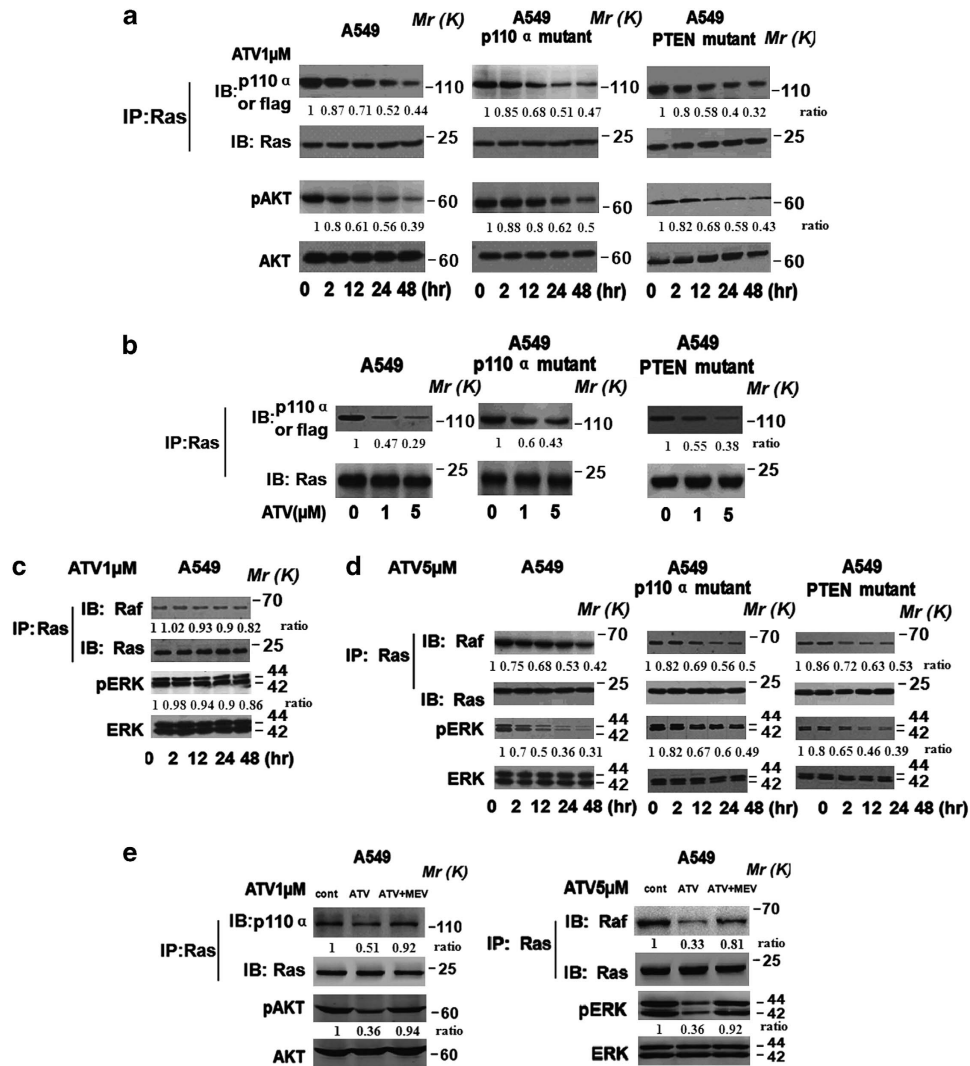


**Figure 5** Atorvastatin disrupts the Kras/PI3K or Kras/Raf complex and subsequently inhibits the AKT or ERK activation in NSCLC cells. (a) A549 cells and their PIK3CA and PTEN mutants were respectively treated with 1  $\mu$ M atorvastatin according to specific time points. Lysates were immunoprecipitated by using anti-Kras antibody and analyzed for coimmunoprecipitating p110 $\alpha$  or flag antibody using western blotting. AKT activity is represented as the levels of phosphorylated forms of AKT compared with total AKT. (b) Dose response of atorvastatin on the Kras/ p110 $\alpha$  complex in A549 cells and their PIK3CA and PTEN mutants. (c) A549 cells were respectively treated with 1  $\mu$ M atorvastatin according to specific time points. Lysates were immunoprecipitated by using anti-Kras antibody and analyzed for coimmunoprecipitating with Raf antibody. ERK activity was represented as the levels of phosphorylated forms of ERK compared with total ERK. (d) A549 cells and their PIK3CA and PTEN mutants were respectively treated with 5  $\mu$ M atorvastatin according to specific time points. The protocols of immunoprecipitation and western blotting were similar to those used above. (e) A549 cells were respectively treated with 1  $\mu$ M or 5  $\mu$ M atorvastatin for 48 h. Administration with 100  $\mu$ M mevalonate reversed the inhibitory effect of atorvastatin on the formation of Kras/PI3K or Kras/Raf complex and the activation of AKT and ERK

A549 cells. As shown in Figure 5b, after a 48-h treatment, atorvastatin also resulted in a dose-dependent dissociation of the PI3K p110 $\alpha$  subunit from Kras in A549 cells, as well as comutant KRAS/PIK3CA or KRAS/PTEN A549 cells, corresponded with inhibition of AKT kinetics determined by means of ELISA assay (Figures 3d, e and f). Consistent results were also obtained in Calu1 cells (Supplementary Figure 1A and B).

As shown in Figure 5c, atorvastatin (1  $\mu$ M) administration had no effects on the interaction of Kras with Raf after 0–48 h incubation, corresponding with failure to inhibit the MEK/ERK pathway in A549 cells. Consistent results were also obtained in Calu1 cells (Supplementary Figure 1C). These results may account for no effects of atorvastatin (1  $\mu$ M) on kinetics of ERK in these cells (Figure 3g). However, as shown in Figure 5d,

when the dose of atorvastatin was increased to 5  $\mu$ M, it could confer a time-dependent dissociation of Raf from Kras corresponding with the inhibition of the MEK/ERK pathway in A549 cells, as well as comutant KRAS/PIK3CA or KRAS/PTEN A549 cells. Consistent results were also obtained in Calu1 cells (Supplementary Figure 1D).

Therefore, the above results together suggest that inhibition of the PI3K/AKT and MEK/ERK pathways by atorvastatin in KRAS mutant NSCLC cells correlates with disruption of the Kras/Raf and Kras/PI3K complexes irrespective of the PIK3CA and PTEN statuses.

To determine whether the effects of atorvastatin on the Kras/Raf and Kras/PI3K complexes are derived from its main function inhibition of HMG-CoA reductase, we added

mevalonate to the culture medium. As shown in Figure 5e, additional mevalonate treatment reversed the effects of atorvastatin on the Kras/Raf and Kras/PI3K complexes, corresponded with inhibition of AKT and ERK activities in A549 cells. Consistent results were also obtained in Calu1 cells (Supplementary Figure 1E).

**Atorvastatin and gefitinib synergize in suppressing tumor growth *in vivo*.** It was critical to determine whether the synergistic effect of atorvastatin and gefitinib could exist *in vivo*. A549 cells, A549 cells harboring PIK3CA mutant or PTEN loss mutant ( $\sim 1 \times 10^6$  cells each group) were subcutaneously inoculated into the right flank of 6-week-old female nude mice. When tumors grew to  $\sim 100 \text{ mm}^3$  in size, the animals were treated with gefitinib (100 mg/per thrice days, oral gavage), clinical dose of atorvastatin (1 or 10 mg/kg/day, daily oral gavage), and gefitinib plus atorvastatin (combination therapy was categorized into two groups: 100 mg/mouse/once every 3 days gefitinib plus 1 mg/kg/day atorvastatin, and 100 mg/mouse/once every 3 days gefitinib plus 10 mg/kg/day atorvastatin), respectively.

To address the long-term survival-prolonging effect of the combination, we further observe the survival rate between control group and different doses of atorvastatin and gefitinib alone and their combination in a cycle of 60 days approximately. As shown in Figure 6a, the survival rate of A549 tumor-bearing nude mice treated with atorvastatin plus gefitinib was significantly increased compared with gefitinib treatment agent alone. Similar results were also obtained in nude mice bearing A549 tumors harboring PIK3CA mutant or PTEN loss.

We also observed the changes of tumor volume after 21-day treatment. As shown in Figure 6b, the combination of gefitinib and atorvastatin resulted in a statistically significantly reduced tumor volume compared with each agent alone, at both low and high doses, respectively. The statistical analysis for tumor volume after 21-day treatment has been shown in Supplementary Figure 2. Similar results were also obtained in nude mice bearing A549 tumors harboring PIK3CA mutant or PTEN loss. Statistical data for Figures 6a and b are shown in Supplementary Tables 1 and 2, respectively. Furthermore, the cytotoxic effect of combination of atorvastatin and gefitinib was further confirmed by Ki67 (the biomarker to evaluate tumor proliferation) (Figure 7a) and TUNEL staining analysis (evaluation of tumor apoptosis) (Figure 7b).

To explore the mechanism underlying the combination efficacy *in vivo*, we performed immunohistochemical staining assay to determine the effect of the combination of atorvastatin and gefitinib on the levels of pAKT and pERK in tumor tissues. After 1-week treatment, treatment with atorvastatin plus gefitinib significantly reduced the levels of pAKT (Figure 8a) and pERK (Figure 8b) compared with each agent alone in A549 tumors or tumors harboring PIK3CA mutant or PTEN loss, respectively. To confirm and quantify such findings, the ELISA assay was performed. As shown in Figures 8c and d, the combination of gefitinib and atorvastatin resulted in statistically significantly reduced levels of pAKT and pERK compared with each agent alone, at both low and high doses, respectively. Similar results were also obtained in nude mice bearing A549 tumors harboring PIK3CA mutant or PTEN loss.

## Discussion

Mutations in the KRAS gene have been found in 20–30% of NSCLC<sup>14</sup> and believed to be critically involved in gefitinib resistance. However, how mutant KRAS mediates gefitinib resistance in NSCLC treatment is still a puzzle. Previous studies have confirmed that mutant Kras directly binds to Raf proteins and the PI3K subunit p110 $\alpha$ , leading to constitutive activation of both the MEK/ERK and PI3K/AKT pathways.<sup>15</sup> In the present study, our data show that transfection of mutant KRAS plasmids into WT NSCLC cell line Calu3 confers gefitinib resistance in these cells. Consistent with other reports,<sup>16,17</sup> this work indicates that gefitinib can efficiently inhibit the activation of AKT and ERK in KRAS WT NSCLC cells, whereas has no effects on the ERK and AKT activities in KRAS mutant NSCLC cells. Specifically, we find that gefitinib has the capacity to inhibit the interaction of Kras with Raf and PI3K in KRAS WT cells, whereas not in KRAS mutant cells. Therefore, combined with the finding that gefitinib shows antitumor activity mainly via the blockage of downstream MEK/ERK and PI3K/AKT signaling pathways,<sup>13</sup> the present study suggests that the failure of gefitinib to disrupt the Kras/Raf and Kras/PI3K complexes contributes to mutant KRAS-mediated gefitinib resistance in NSCLC cells.

RAS has been found to activate several other effector pathways, the two best characterized of which are the Raf/MAPK and PI3K/AKT pathways.<sup>1</sup> Knockdown of mutant KRAS results in decreased ERK activity in various NSCLC cell lines, and reduces the AKT activity in KRAS-dependent NSCLC cells (H358 cells), whereas enhances or has minimal effect on the AKT activity in KRAS-independent A549 NSCLC cells, respectively.<sup>18,19</sup> Similar results were reported that mutant KRAS knockdown suppresses ERK and AKT activities in the KRAS-dependent SW620 colon cancer cells, while reduces ERK activity but increases AKT activity in the KRAS-independent SW837 cells.<sup>20</sup> In the present study, however, we find that atorvastatin-induced inhibition of ERK and AKT activities may be, at least partly, derived from its disruption of the interaction of Kras with Raf and PI3K in NSCLC cells including KRAS-independent A549 cells. These results suggest that disturbance of direct interaction of Kras with Raf and PI3K reduces ERK and AKT activities in both KRAS-dependent and -independent NSCLC cells. The discrepancy of our results with others may be due to the fact that knockdown of mutant KRAS can influence other genes' expression, for example IL-8.<sup>21</sup> This effect may vary in different cancer cell lines and some factors affected by mutant KRAS knockdown may subsequently enhance AKT activity in certain cancer cells. Furthermore, our data show that atorvastatin can also disrupt the Kras/Raf and Kras/PI3K complexes in comutant KRAS/PIK3CA and KRAS/PTEN NSCLC cells, leading to decreased ERK and AKT activities. These results suggest that the interaction of mutant Kras to Raf and PI3K is still critically involved in regulation of its downstream ERK and AKT activities irrespective of the PIK3CA and PTEN statuses.

Statins have been confirmed to exhibit pro-apoptotic and growth-inhibitory responses in neoplastic cells of diverse origin. For example, Mistafa *et al.*<sup>22</sup> reported that statins inhibit the growth of pancreatic cancer cells via P2  $\times$  7 receptor-mediated inhibition of AKT signaling. Yanae *et al.*<sup>23</sup> reported



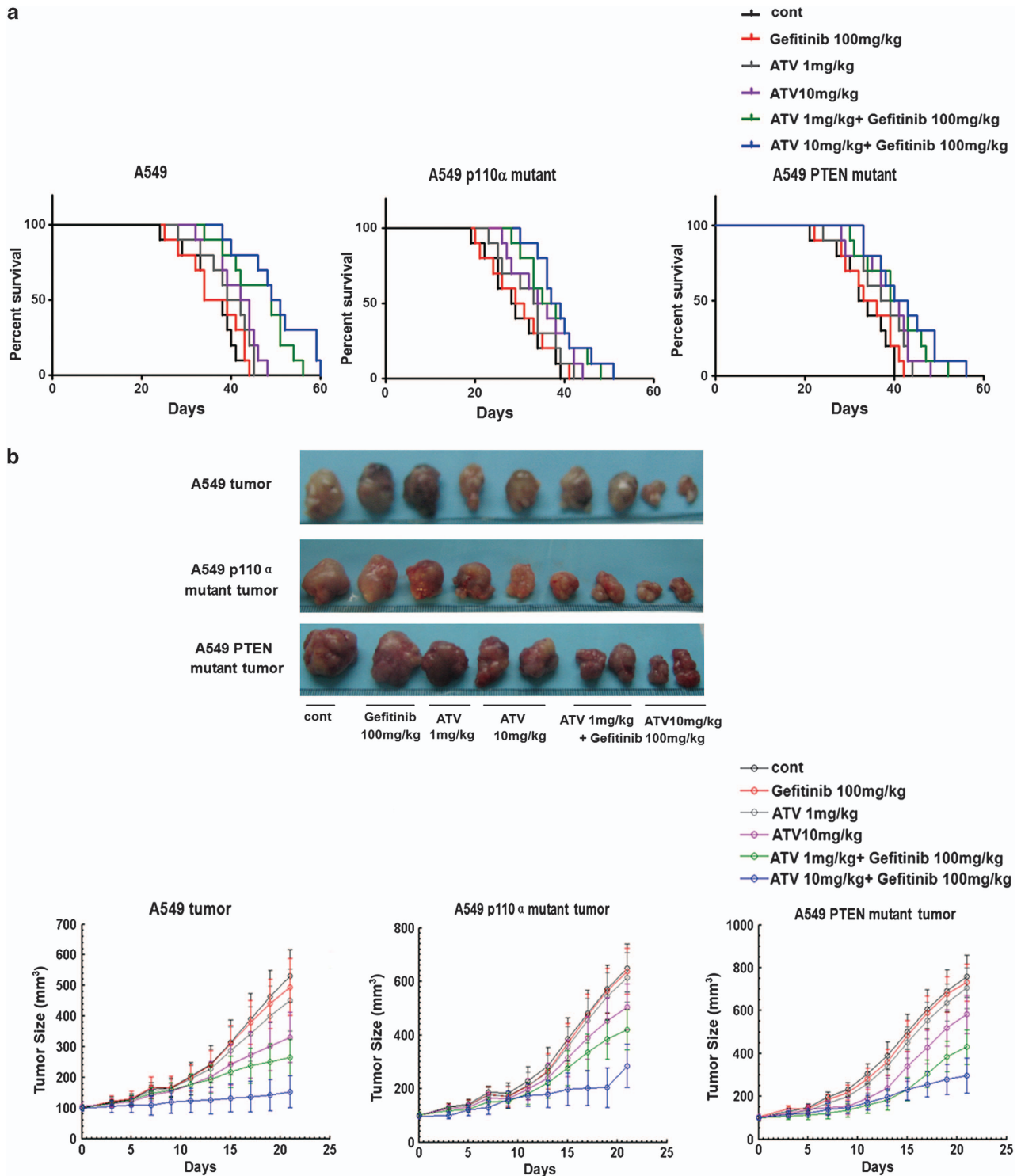


**Figure 6** Effects of atorvastatin (ATV) on antitumor activity of gefitinib in nude mice bearing human lung cancer A549 and its PIK3CA or PTEN mutant xenografts. (a) Kaplan–Meier curves for illustration of the survival periods of xenograft-bearing mice treated with atorvastatin (1 mg/kg/day, p.o.) and gefitinib (100 mg/kg, thrice a week, p.o.), atorvastatin (10 mg/kg/day, p.o.) and gefitinib (100 mg/kg, thrice a week, p.o.) and each agents alone. The day 0 was used to represent the starting of treatment. (b) Representative A549 or its PIK3CA and PTEN mutant xenograft tumors resected on day 21 showing the difference in tumor volumes between individual agents and their combinations. The lower panel of b, tumor size was measured every 2 days for the indicated period. The treatment period was 21 days. Control mice received the vehicle. *P*-value was determined by log-rank test. Ten mice per group, mean  $\pm$  S.D. Also see Supplementary Tables 1 and 2, respectively

that statins induce apoptosis via inhibition of the geranylgeranyl-pyrophosphate biosynthesis and resultant suppression of ERK and Akt activation in glioblastoma cell. The present

study finds that atorvastatin itself has obvious capacity to induce NSCLC cell apoptosis and inhibit cell proliferation. Besides, atorvastatin administration efficiently suppresses

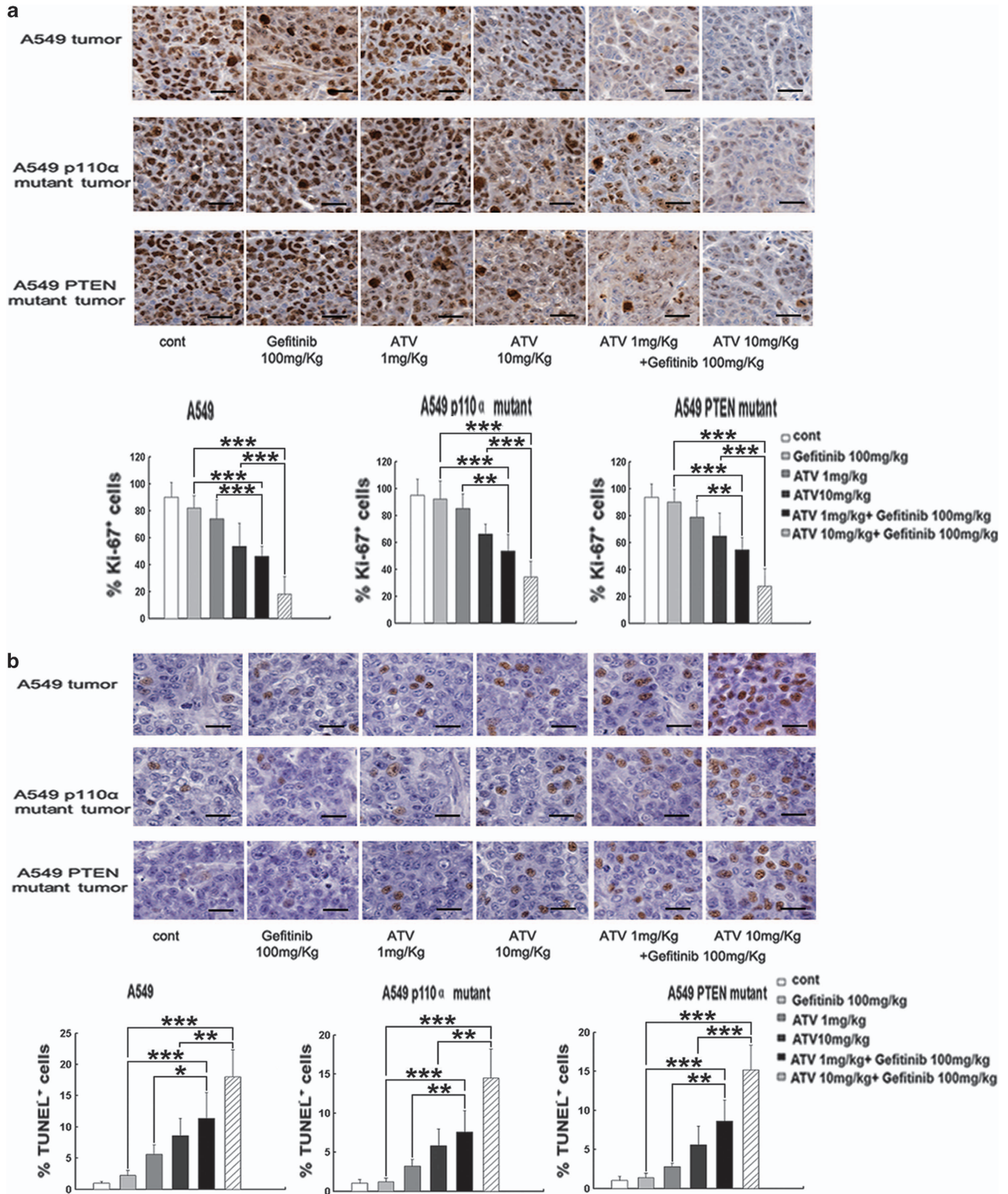


**Figure 7** Effects of atorvastatin and gefitinib alone or in combination on the biomarkers of the growth and apoptosis of A549 or its PIK3CA and PTEN mutant tumor *in vivo*. (a) The positive staining of Ki67 expression per field from paraffin-embedded sections of A549 and its PIK3CA or PTEN mutant tumor treated with either atorvastatin or gefitinib alone or in combination was determined by immunohistochemistry and morphometric quantification. (b) Apoptotic nuclei with fragmented DNA were detected by TUNEL staining, and further analyzed by morphometric quantification. The final statistical graphs represent 10 non-overlapping images of each tumor specimen from five animals per group. All scale bars represent 50  $\mu$ m. \* $P < 0.05$ ; \*\* $P < 0.01$ ; \*\*\* $P < 0.001$

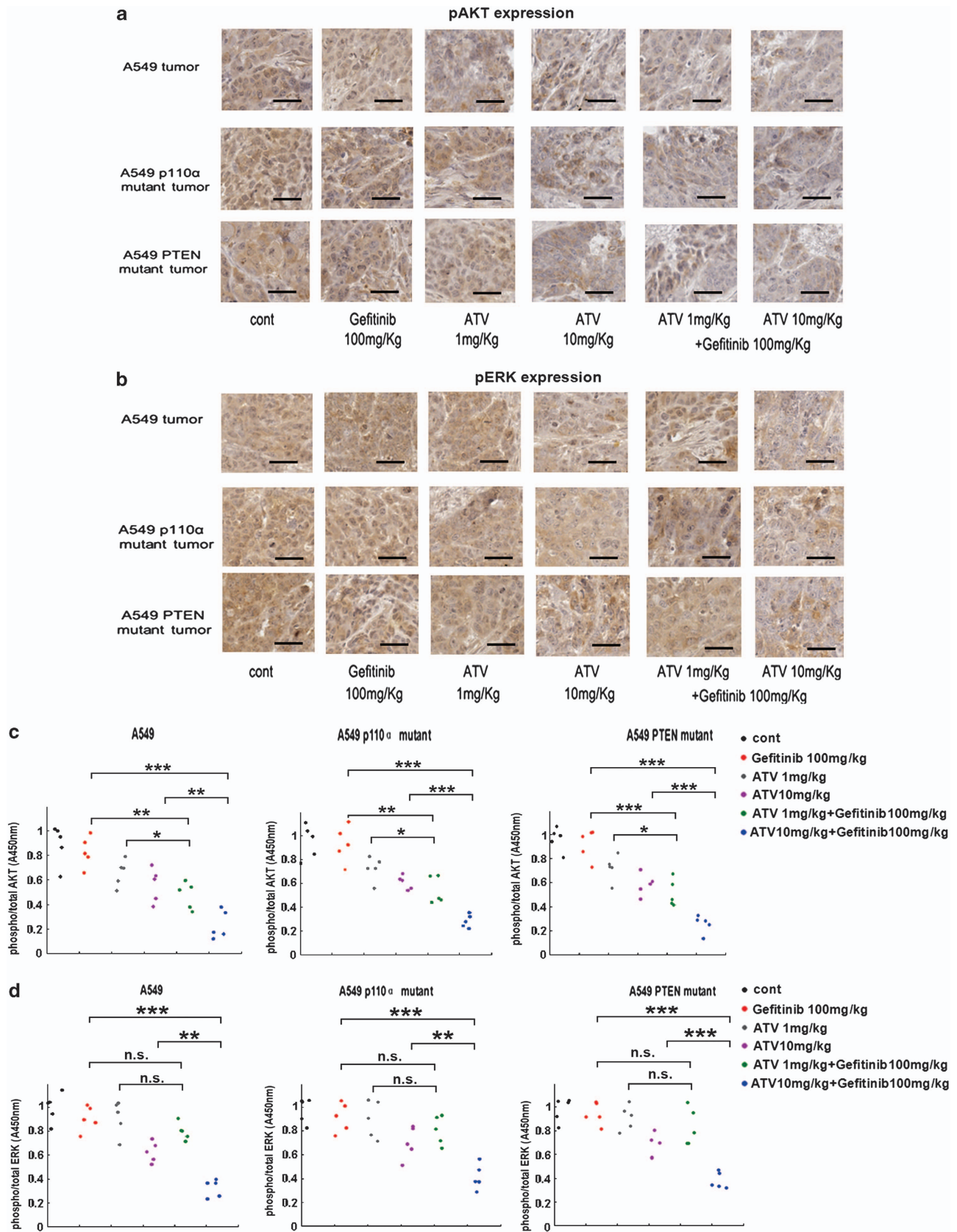


**Figure 8** Effects of atorvastatin and gefitinib alone or in combination on the activation of AKT and ERK of A549 or its PIK3CA and PTEN mutant tumors *in vivo*. (a and b) pAKT (a) and pERK (b) expression levels were analyzed for immunohistochemistry and the ratio of pAKT and total AKT (c) or pERK and total ERK (d) by using ELISA assay. Scatterplots represented five independent experiments in per group. All scale bars represent 50  $\mu$ m. n.s., no significant difference. \* $P < 0.05$ ; \*\* $P < 0.01$ ; \*\*\* $P < 0.001$

ERK and AKT activation, mainly due to disruption of Kras/Raf and Kras/PI3K complexes in NSCLC cells. The results that mevalonate administration reverses the effects of atorvastatin on Kras/Raf and Kras/PI3K complexes suggest that atorvastatin disrupts Kras/Raf and Kras/PI3K complexes in NSCLC cells through inhibition of HMG-CoA reductase.

These data together suggest that inhibition of the MEK/ERK and PI3K/AKT pathways is closely related to the antitumor activity of statins in various tumors. Furthermore, our results suggest that blockage of interaction of mutant Kras to Raf and PI3K may contribute to a critical molecular mechanism underlying the statins-mediated antitumor effect.

The present study shows that atorvastatin at the relative low dose (1  $\mu$ M) works effectively to disrupt the direct interaction of Kras with PI3K but not Raf, whereas a high dose (5  $\mu$ M) of atorvastatin can inhibit the interaction of mutant Kras to Raf. The possible explanation for these effects may be that the affinity of the Ras/Raf complex is higher than that of the Ras/PI3K complex.<sup>24</sup> This explanation may also clarify our previous finding that atorvastatin sensitizes human NSCLC cells to carboplatin via the suppression of AKT but not ERK signaling,<sup>12</sup> as 2.5  $\mu$ M atorvastatin used in such study is not sufficient to disturb the Kras/Raf complex in NSCLC cells.

Combining statins and TKIs showed enhanced inhibition and cooperative cytotoxicity in a variety of cancer cell lines.<sup>10,25</sup> Specifically in NSCLC cells, Park *et al.*<sup>26</sup> reported that lovastatin overcomes gefitinib resistance in these cells with KRAS mutations by downregulation of the RAS protein, leading to inhibition of both MEK/ERK and PI3K/AKT pathways. In such a study, lovastatin was confirmed to reduce RAS protein expression, but inhibit AKT activity in KRAS-independent A549 and H460 NSCLC cells. These results seem inconsistent with that knockdown of mutant KRAS enhances or has minimal effect on the AKT activity in KRAS-independent A549 NSCLC cells as mentioned above. The possible reason may be that lovastatin may also disrupt the Kras/Raf and Kras/PI3K complexes, which makes the effect of lovastatin on AKT activity in these cells complicated. This study combined with ours also suggests that disruption of the direct interaction of Kras with Raf and PI3K may partly account for atorvastatin-mediated inhibition of ERK and AKT activities, and resultant enhancement of gefitinib efficacy in NSCLC cells.

KRAS mutation frequently co-occurs with PTEN loss-of-function mutation or PIK3CA mutation in lung cancer cells. However, mutations in both RAS and BRAF as well as PIK3CA and PTEN are rarely concurrent in the same tumor.<sup>27–29</sup> In the present study, besides in KRAS mutant NSCLC cells, we also find that atorvastatin can overcome gefitinib resistance in comutant KRAS/PIK3CA and KRAS/PTEN NSCLC cells. Therefore, our work suggests that atorvastatin can overcome gefitinib resistance in KRAS mutant NSCLC cells irrespective of the PTEN and PIK3CA statuses.

Overall, our results have a number of general implications. We have defined the mechanism of mutant tumor biomarker (KRAS)-mediated shifting signaling inhibitory effect of gefitinib through Kras interacting with PI3K or Raf. We design a therapeutic schedule of atorvastatin plus gefitinib, which could effectively exert a cytotoxic effect on the KRAS mutant NSCLC tumors under various conditions and more substantially prolong the survival rate in preclinical study.

## Materials and Methods

**Cell lines, plasmids, and transfection.** Human NSCLC cell lines (originally purchased from ATCC) with documented KRAS mutations-A549 (KRAS G12S), Calu1 (KRAS G12C), H460 (KRAS Q61H PIK3CA E545K), H157 (KRAS G12R PTEN G251C), and one KRAS WT NSCLC cell-Cal3 were used. The procedure of transfection of pBabe puro-KRAS G12V (Addgene, Cambridge, MA, USA; Plasmid 9052) and the corresponding empty vector pBabe puro was strictly according to a previous report.<sup>30</sup> Human TrueORF PIK3CA E545K plasmid was purchased from OriGene Technologies (Rockville, MD, USA; Cat. no. RC400348). TrueORFs have a C-terminal fusion of MYC/DDK tag. The cloning expression vector is pCMV6-Entry, A549 and Calu1 cells were stably transfected with PIK3CA E545K according to another work.<sup>31</sup> For shRNA experiments, cells stably transfected with the pRetroSuper (pRS; OriGene) and pRS vector expressing shRNA for PTEN knockdown (pRS-shPTEN; OriGene; Cat. no. TR320498) were performed as that previously reported.<sup>32</sup>

**Cell proliferation/viability assay, flow cytometry (FCM) analysis of apoptosis and caspase activity assay.** The protocols and reagents used for MTT assay (detection of cell proliferation/viability), flow cytometry analysis of apoptosis, and Caspase 3/7 activity assays were all strictly according to our previous work.<sup>12</sup>

**Immunoprecipitation.** Immunoprecipitation was performed according to a previous study.<sup>33</sup> Cells were treated with atorvastatin (1 or 5  $\mu$ M) according to specific time points, and then scraped into ice-cold PBS and lysed with lysis buffer. The cell lysates were incubated with monoclonal anti-Kras antibody (Sigma, St. Louis, MO, USA; Cat. no. WH0003845M1) then precipitated the resultant immune complexes with protein A-sepharose beads (Amersham Biosciences, Arlington Heights, IL, USA). The immunoprecipitated material was washed and pellets were resuspended in SDS sample buffer and subjected to western blotting analysis.

**Western blotting.** Western blotting protocol was as that previously reported with minor modifications.<sup>34</sup> Cells were first seeded at a concentration of  $1 \times 10^6$  cells per 100-mm dish (Corning, Corning, NY, USA), incubated at 37 °C for 1 day, and then incubated with atorvastatin (1 or 5  $\mu$ M) for specific times. For Western blotting analysis of AKT (Cat. no. 9272), pAKT (Cat. no. 4060), ERK (Cat. no. 4695), pERK (Cat. no. 4370), PTEN (Cat. no. 9188), and PI3K p110 $\alpha$  (Cat. no. 4249), blots were probed with their specific antibodies (diluted with 5% BSA to 1:1000; all antibodies from Cell Signaling, Boston, MA, USA), respectively. The mouse monoclonal anti-flag antibody (diluted with 5% BSA to 1:5000; Sigma-Aldrich, St. Louis, MI, USA) was used to recognize the DDK tag of PIK3CA E545K.

**Confocal microscopy.** Cells seeded on chamber slides were briefly washed with PBS and fixed with cold 100% methanol for 5 min. The slides were then subjected to a series of steps according to the previous study, except for the appropriate primary antibodies used in the present study. Cell nuclei were stained with DAPI (1:10 000 dilutions in PBS). The glass coverslips were mounted with 50% glycerol (in PBS, pH7.6) and examined under a fluorescence microscope with appropriate filters.<sup>35</sup>

**ELISA analysis.** ELISA analysis both *in vitro* and *in vivo* using the ELISA analysis kits (pAKT: Cat. no. 7160, CST; AKT: Cat. no. 7170, CST; pERK: Cat. no. 7315, CST; ERK: Cat. no. 7050, CST) according to the manufacturer's instructions. For analysis of AKT and ERK activation *in vitro*, cells were first treated with atorvastatin (1 or 5  $\mu$ M), gefitinib (1  $\mu$ M), or their combinations for 48 h. For analysis of AKT and ERK activation *in vivo*, tumor-bearing nu/nu mice were treated with atorvastatin 1 or 10 mg/kg, gefitinib 100 mg/kg and their combinations or control solvent for 1 week. Tumors were snapped frozen and homogenized in cell lysis buffer (CST; Cat. no. 9803). Ratios of pAKT to total AKT and pERK to total ERK were determined by specific ELISA assays.

**Xenograft studies.** Animal handling and procedures were approved by the Qiqihar Medical University Animal Care and Use Committee. Xenograft studies were strictly according to our previous report<sup>12</sup>, except drug treatment.

**TUNEL staining.** The TUNEL staining was performed according to the manufacturer's instructions of *In situ* cell death detection kit (Roche, Basel, Switzerland). After 15-min incubation with Proteinase K (20 mg/ml) at room temperature, the sections were incubated with 2% H<sub>2</sub>O<sub>2</sub> for 5 min for blocking endogenous peroxidase. Then sections were incubated with the TdT enzyme at 37 °C for 2 h. After 30-min incubation with antidigoxin-peroxidase solution, the sections were stained with diaminobenzidine (DAB) substrate for 2 min and then counterstained with hematoxylin. Thereafter, slides were photographed with a microscope camera system.

**Immunohistochemistry.** The immunostaining assay was performed as previously described.<sup>32</sup> Tissues harvested from A549 and its PIK3CA or PTEN mutant tumors were fixed in 10% formaldehyde overnight and then embedded in paraffin. After deparaffinization, hydration and blockage of endogenous peroxidase routinely, sections were pretreated by microwaving for 20 min in Tris-EDTA (pH 9.0) buffer for antigen retrieval. The slides were blocked with 5% goat serum at room temperature for 1 h and then incubated with antibody against pAKT and pERK overnight at 4 °C, followed by incubation with horseradish peroxidase-conjugated secondary antibodies for 1 h at room temperature. Slides were counterstained with hematoxylin, then photographed and converted into a digital image using light microscopy equipped with camera.

**Statistical analysis.** All statistical analyses were evaluated by Student's *t*-test for simple comparisons between two groups and one-way ANOVA for comparisons among multiple groups using GraphPad Prism version 5.0 (GraphPad Software Inc, La Jolla, CA, USA) and JMP7.0 software (SAS Institute Inc, Cary, NC, USA). In MTT assay, the half-maximal inhibitory concentration (IC<sub>50</sub>) was calculated using SPSS 12.0 software (SPSS Inc, Chicago, IL, USA). Kaplan–Meier analysis was used to plot overall survival and differences in curves were analyzed by log-rank test. All tests were two-sided and expressed as mean ± S.D. A *P*-value of <0.05 was considered significant.

### Conflict of Interest

The authors declare no conflict of interest.

**Acknowledgements.** This work was supported by the National Natural Science Foundation of China (No.81201622, 81173609, 81202084, 30973902) and Province Natural Science Foundation of Hei Long Jiang (No. D200929, D201027).

### Author contributions

JC, BL, and JL conceived and designed the experiments. JC, HB, JH, XZ, CZ, LY, XW, DL, HS, JY, and BL performed the experiments. JC, HB, JH, and BL analyzed the data. JC, BL, and JL wrote the paper.

- Downward J. Targeting RAS signalling pathways in cancer therapy. *Nat Rev Cancer* 2003; **3**: 11–22.
- Pao W, Wang TY, Riely GJ, Miller VA, Pan Q, Ladanyi M *et al*. KRAS mutations and primary resistance of lung adenocarcinomas to gefitinib or erlotinib. *PLoS Med* 2005; **2**: e17.
- Cox AD, Der CJ. Ras family signaling: therapeutic targeting. *Cancer Biol Ther* 2002; **1**: 599–606.
- Engelman JA, Mukohara T, Zejnullahu K, Lifshits E, Borras AM, Gale C M *et al*. Allelic dilution obscures detection of a biologically significant resistance mutation in EGFR-amplified lung cancer. *J Clin Invest* 2006; **116**: 2695–2706.
- Yamamoto C, Basaki Y, Kawahara A, Nakashima K, Kage M, Izumi H *et al*. Loss of PTEN expression by blocking nuclear translocation of EGR1 in gefitinib-resistant lung cancer cells harboring epidermal growth factor receptor-activating mutations. *Cancer Res* 2010; **70**: 8715–8725.
- Yoon YK, Kim H P, Han SW, Oh do Y, Im SA, Bang Y J *et al*. KRAS mutant lung cancer cells are differentially responsive to MEK inhibitor due to AKT or STAT3 activation: implication for combinatorial approach. *Mol Carcinog* 2010; **49**: 353–362.
- Chaft JE, Arcila ME, Paik PK, Lau C, Riely GJ, Pietanza MC *et al*. Coexistence of PIK3CA and other oncogene mutations in lung adenocarcinoma—rationale for comprehensive mutation profiling. *Mol Cancer Ther* 2012; **11**: 485–491.
- Goldstein JL, Brown MS. Regulation of the mevalonate pathway. *Nature* 1990; **343**: 425–430.
- Konstantinopoulos PA, Karamouzis MV, Papavassiliou AG. Post-translational modifications and regulation of the RAS superfamily of GTPases as anticancer targets. *Nat Rev Drug Discov* 2007; **6**: 541–555.
- Lee J, Lee I, Han B, Park JO, Jang J, Park C *et al*. Effect of simvastatin on cetuximab resistance in human colorectal cancer with KRAS mutations. *J Natl Cancer Inst* 2011; **103**: 674–688.
- Zheng X, Cui XX, Avila GE, Huang MT, Liu Y, Patel J *et al*. Atorvastatin and celecoxib inhibit prostate PC-3 tumors in immunodeficient mice. *Clin Cancer Res* 2007; **13**: 5480–5487.
- Chen J, Lan T, Hou J, Zhang J, An Y, Tie L *et al*. Atorvastatin sensitizes human non-small cell lung carcinomas to carboplatin via suppression of AKT activation and upregulation of TIMP-1. *Int J Biochem Cell Biol* 2012; **44**: 759–769.
- Ono M, Hirata A, Kometani T, Miyagawa M, Ueda S, Kinoshita H *et al*. Sensitivity to gefitinib (Iressa, ZD1839) in non-small cell lung cancer cell lines correlates with dependence on the epidermal growth factor (EGF) receptor/extracellular signal-regulated kinase 1/2 and EGF receptor/Akt pathway for proliferation. *Mol Cancer Ther* 2004; **3**: 465–472.
- Aviel-Ronen S, Blackhall FH, Shepherd FA, Tsao MS. K-ras mutations in non-small-cell lung carcinoma: a review. *Clin Lung Cancer* 2006; **8**: 30–38.
- Rodriguez-Viciana P, Warne PH, Dhand R, Vanhaesebroeck B, Gout I, Fry MJ *et al*. Phosphatidylinositol-3-OH kinase as a direct target of Ras. *Nature* 1994; **370**: 527–532.
- Janmaat ML, Rodriguez JA, Gallegos-Ruiz M, Kruyt FA, Giaccone G. Enhanced cytotoxicity induced by gefitinib and specific inhibitors of the Ras or phosphatidylinositol-3 kinase pathways in non-small cell lung cancer cells. *Int J Cancer* 2006; **118**: 209–214.
- Janmaat ML, Kruyt FA, Rodriguez JA, Giaccone G. Response to epidermal growth factor receptor inhibitors in non-small cell lung cancer cells: limited antiproliferative effects and absence of apoptosis associated with persistent activity of extracellular signal-regulated kinase or Akt kinase pathways. *Clin Cancer Res* 2003; **9**: 2316–2326.
- Sunaga N, Shames DS, Girard L, Peyton M, Larsen JE, Imai H *et al*. Knockdown of oncogenic KRAS in non-small cell lung cancers suppresses tumor growth and sensitizes tumor cells to targeted therapy. *Mol Cancer Ther* 2011; **10**: 336–346.
- Singh A, Greninger P, Rhodes D, Koopman L, Violette S, Bardeesy N *et al*. A gene expression signature associated with “K-Ras addiction” reveals regulators of EMT and tumor cell survival. *Cancer Cell* 2009; **15**: 489–500.
- Singh A, Sweeney MF, Yu M, Burger A, Greninger P, Benes C *et al*. TAK1 inhibition promotes apoptosis in KRAS-dependent colon cancers. *Cell* 2012; **148**: 639–650.
- Sunaga N, Imai H, Shimizu K, Shames DS, Kakegawa S, Girard L *et al*. Oncogenic KRAS-induced interleukin-8 overexpression promotes cell growth and migration and contributes to aggressive phenotypes of non-small cell lung cancer. *Int J Cancer* 2012; **130**: 1733–1744.
- Mistafa O, Stenius U. Statins inhibit Akt/PKB signaling via P2 × 7 receptor in pancreatic cancer cells. *Biochem Pharmacol* 2009; **78**: 1115–1126.
- Yanae M, Tsubaki M, Satou T, Itoh T, Imano M, Yamazoe Y *et al*. Statin-induced apoptosis via the suppression of ERK1/2 and Akt activation by inhibition of the geranylgeranyl-pyrophosphate biosynthesis in glioblastoma. *J Exp Clin Cancer Res* 2011; **30**: 74.
- Herrmann C. Ras-effector interactions: after one decade. *Curr Opin Struct Biol* 2003; **13**: 122–129.
- Cemeus C, Zhao TT, Barrett GM, Lorimer IA, Dimitroulakos J. Lovastatin enhances gefitinib activity in glioblastoma cells irrespective of EGFRvIII and PTEN status. *J Neurooncol* 2008; **90**: 9–17.
- Park IH, Kim JY, Jung J I, Han JY. Lovastatin overcomes gefitinib resistance in human non-small cell lung cancer cells with K-Ras mutations. *Invest New Drugs* 2010; **28**: 791–799.
- Brose MS, Volpe P, Feldman M, Kumar M, Rishi I, Gerrero R *et al*. BRAF and RAS mutations in human lung cancer and melanoma. *Cancer Res* 2002; **62**: 6997–7000.
- Gorden A, Osman I, Gai W, He D, Huang W, Davidson A *et al*. Analysis of BRAF and N-RAS mutations in metastatic melanoma tissues. *Cancer Res* 2003; **343**: 425–430.
- Yuan TL, Cantley LC. PI3K pathway alterations in cancer: variations on a theme. *Oncogene* 2008; **27**: 5497–5510.
- Ji Z, Mei FC, Xie J, Cheng X. Oncogenic KRAS activates hedgehog signaling pathway in pancreatic cancer cells. *J Biol Chem* 2007; **282**: 14048–14055.
- Hung TM, Hu RH, Ho C M, Chiu YL, Lee JL, Jeng YM *et al*. Downregulation of alpha-fetoprotein expression by LHX4: a critical role in hepatocarcinogenesis. *Carcinogenesis* 2011; **32**: 1815–1823.
- Ahn BY, Elwi AN, Lee B, Trinh DL, Klimowicz AC, Yau A *et al*. Genetic screen identifies insulin-like growth factor binding protein 5 as a modulator of tamoxifen resistance in breast cancer. *Cancer Res* 2010; **70**: 3013–3019.
- Junttila TT, Akita RW, Parsons K, Fields C, Lewis Phillips GD, Friedman LS *et al*. Ligand-independent HER2/HER3/PI3K complex is disrupted by trastuzumab and is effectively inhibited by the PI3K inhibitor GDC-0941. *Cancer Cell* 2009; **15**: 429–440.
- Liu B, Wang G, Yang J, Pan X, Yang Z, Zang L. Berberine inhibits human hepatoma cell invasion without cytotoxicity in healthy hepatocytes. *PLoS ONE* 2011; **6**: e21416.
- Liang K, Esteva FJ, Albarracín C, Stemke-Hale K, Lu Y, Bianchini G *et al*. Recombinant human erythropoietin antagonizes trastuzumab treatment of breast cancer cells via Jak2-mediated Src activation and PTEN inactivation. *Cancer Cell* 2010; **18**: 423–435.



**Cell Death and Disease** is an open-access journal published by Nature Publishing Group. This work is licensed under a Creative Commons Attribution-NonCommercial-NoDerivs 3.0 Unported License. To view a copy of this license, visit <http://creativecommons.org/licenses/by-nc-nd/3.0/>

Supplementary Information accompanies this paper on Cell Death and Disease website (<http://www.nature.com/cddis>)